Geophysical Research Letters

RESEARCH LETTER
10.1029/2020GL091505

Impact of the Boreal Summer Intraseasonal Oscillation on Typhoon Tracks in the Western North Pacific and the Prediction Skill of the ECMWF Model

M. Nakano[1], **F. Vitart**[2], **and K. Kikuchi**[3]

[1]Japan Agency for Marine-Earth Science and Technology, Yokohama, Japan, [2]European Centre for Medium-Range Weather Forecasts, Reading, UK, [3]International Pacific Research Centre, University of Hawai'i, Honolulu, USA

Key Points:

- The impact of the boreal summer intraseasonal oscillation on the typhoon tracks varies month to month
- The European Centre for Medium-Range Weather Forecasts model successfully reproduces the impact up to a month in advance
- Reproduction of modulations in the typhoon genesis location leads to accurate tropical cyclone track forecasts

Supporting Information:

Supporting Information may be found in the online version of this article.

Correspondence to:

M. Nakano,
masuo@jamstec.go.jp

Citation:

Nakano, M., Vitart, F., & Kikuchi, K. (2021). Impact of the boreal summer intraseasonal oscillation on typhoon tracks in the Western North Pacific and the prediction skill of the ECMWF model. *Geophysical Research Letters*, *48*, e2020GL091505. https://doi.org/10.1029/2020GL091505

Received 2 NOV 2020
Accepted 10 APR 2021

Abstract The tropical intraseasonal oscillation (ISO) strongly influences tropical cyclone (TC) genesis. However, little is known concerning its impact on TC tracks. Here, we examine how TC tracks in the western North Pacific are modulated by the boreal summer ISO (BSISO) during each month of the TC season (June–October) using the best track data and how well the modulation are reproduced in the European Centre for Medium-Range Weather Forecasts (ECMWF) model forecasts. The results reveal that the impact of the BSISO on the typhoon tracks varies month to month. The ECMWF model successfully reproduces this impact up to a month in advance. A simple advection model shows that the reproduction of the modulations in the TC genesis location leads to accurate TC track forecasts. These results suggest that the BSISO is one of the major sources of TC track predictability at the subseasonal time scale (2 weeks to 2 months).

Plain Language Summary A 30–90-day oscillation of convective activity in the tropical atmosphere affects the formation of tropical cyclones (TCs) in the western North Pacific (WNP) in summer. However, how this oscillation modulates the TC tracks is not yet well documented. In this study, we analyze the observational data and how well the modulation is simulated by a state-of-the-art operational numerical weather prediction model to discuss further improvements in TC predictions beyond 2 weeks that are necessary to mitigate the risk of TCs. The results show that the modulation of the TC track by the oscillation varies month to month. For example, TCs formed in the enhanced convection phases in the WNP have a lower chance of hitting Japan than those formed in the suppressed phases in September. In October, however, TCs formed in the enhanced phases have a higher chance of hitting Japan. The model can simulate the TC track modulation well in June, July, and September but not in August and October. Further detailed analyses suggest that model error in the modulation of the TC formation distribution caused by the oscillation causes errors in the TC tracks. These findings will help further improvement of the TC predictions beyond 2 weeks.

1. Introduction

Observational studies have shown that the 30–90-day-period intraseasonal oscillation (ISO) in the tropical atmosphere strongly influences tropical cyclone (TC) activity (Kikuchi & Wang, 2010; Klotzbach, 2014; Liebmann et al., 1994; Nakazawa, 2006; Yoshida et al., 2014). Previous model studies have shown that the ISO is a major source of predictability for TC activity at subseasonal (2 week to 2 month) time scales (Nakano et al., 2015; Vitart, 2009). In the western North Pacific (WNP), the most active basin of TC activity on the globe, Yoshida et al. (2014) showed that more TCs form in the enhanced convective phases of the boreal summer ISO (BSISO; Kikuchi, 2021; Kikuchi et al., 2012; Wang & Rui, 1990; Wang & Xie, 1997) while less TCs form in the suppressed convective phases. Nakano et al. (2015) showed that a successful simulation of the eastward extension of the monsoon trough in the WNP associated with the enhanced convective phases of the BSISO leads to accurate TC genesis forecasts using a cloud system-resolving model.

Understanding the dynamic background of TC track predictability at subseasonal time scales and improving the numerical weather prediction models are essential to mitigate the risk and impact of TCs. Previous studies have shown that TC tracks in the WNP are influenced by background fields such as the WNP subtropical high and monsoon trough (Camargo et al. 2007; Harr & Elsberry 1991, 1995), as well as the BSISO (Li & Zhou, 2013). However, these studies were based on the means of the entire typhoon season (e.g.,

June–November). Considering that the BSISO behavior is affected by background fields, such as the vertical wind shear (Jiang et al., 2004; Wang & Xie, 1997), which may be influenced by the monsoon trough and subtropical high, and that the large-scale field varies considerably month to month in boreal summer in the WNP (Hirata & Kawamura, 2014; Kawatani et al., 2008), the impact of the BSISO may also change from month to month. Here, we examine how TC tracks in the WNP are modulated by the BSISO for each month of the TC season (June−October) using the best track data and how well the modulation is reproduced in the European Centre for Medium-Range Weather Forecasts (ECMWF) model.

2. Method and Data

The ECMWF model data were produced using the Integrated Forecasting System (IFS) Cy43r3 and are available from the Subseasonal to Seasonal prediction project (S2S) database (Vitart et al., 2017). The data consist of an 11-member ensemble of 46-day forecasts produced twice a week. The forecast data initialized in the period of 1998–2016 were analyzed and compared with observations over the same period.

The BSISO phase and amplitude were calculated using the real-time monitoring method proposed by Kikuchi et al. (2012; see Section 6), which is based on an extended empirical orthogonal function analysis (Weare & Nasstrom, 1982) for three time steps (days −10, −5, and 0) of the outgoing longwave radiation (OLR) in boreal summer (June−August). National Oceanic and Atmospheric Administration OLR data (Liebmann & Smith, 1996) were used as the observations. Kikuchi et al. (2012) calculated the OLR anomaly by subtracting the climatological mean and the three harmonics of the climatological seasonal cycle. To treat the observations and the model simulations in the same manner, the observed OLR anomaly was calculated by subtracting the daily climatology, which was linearly interpolated from the monthly climatology. The seasonal cycle of the interpolated daily climatology from the monthly climatology was very similar to that calculated by the method used in Kikuchi et al. (2012). The model OLR anomaly was calculated by subtracting the model climatology, which was calculated on a monthly basis and then interpolated to the model initial date. Therefore, the model bias, which generally grows with the forecast lead time, was also subtracted. In this study, we defined phases 5–8 as the enhanced BSISO phases and phases 1–4 as the suppressed BSISO phases in the WNP. The phases were defined in the observations and in the model. The accuracy of the predicted BSISO phases and amplitudes was not considered in this study, which instead focuses on how the model accurately reproduces the impact of the BSISO.

Observed TC tracks were retrieved from the International Best Track Archive for Climate Stewardship (IBTrACS; Knapp et al., 2010) v03r10. TCs are considered to have formed at the time when the storms reach tropical storm intensity (maximum surface wind speed >34 kt). In the ECMWF model, storms are tracked using the method proposed by Vitart et al. (1997), which searches for the low-level vortex and sea surface pressure minimum associated with a warm core structure. Storms that retain a maximum surface wind speed higher than 25 kt for at least 2 days are regarded as TCs in the model. TCs in the model detected at the initial date were excluded from the analysis to avoid contamination by pre-existing TCs that formed prior to the model initial date. These thresholds were determined using the TC frequency averaged over the TC season (0.111 day^{-1}), which is similar to the observed frequency (0.116 day^{-1}). TCs formed in the WNP (100–180°E, 0–25°N) were analyzed both in the observations and in the model. To focus on the impact of the BSISO on the TC track, the TC track density for TCs formed in the enhanced and suppressed BSISO phases within a certain forecast lead week were normalised by the number of TCs formed in each respective BSISO phase; then, the difference in the normalised TC track density between the enhanced and suppressed BSISO phases was analyzed.

The TC motion was determined according to the large-scale advecting flow (steering flow) and the interaction between TCs and the large-scale flow including the planetary vorticity (the beta effect; Holland, 1983). To discuss the source of the model error, a beta and advection model (BAM) was used. In BAM, the TC tracks are determined by the beta effect and the steering flow, which is the average of the horizontal wind in the vertical (850–200 hPa) and horizontal (10° × 10° centered on each grid) directions. Marks (1992) estimated the beta effect with angles ranging from 295° to 315° and speeds ranging from 1 to 3 m s^{-1}. Colbert and Soden (2012) used a constant angle of 315° and a variable speed of 1.5–5 m s^{-1} in their experiments. We assume that the effect is constant; TCs are translated with a speed of 2.5 m s^{-1} in the 315° direction

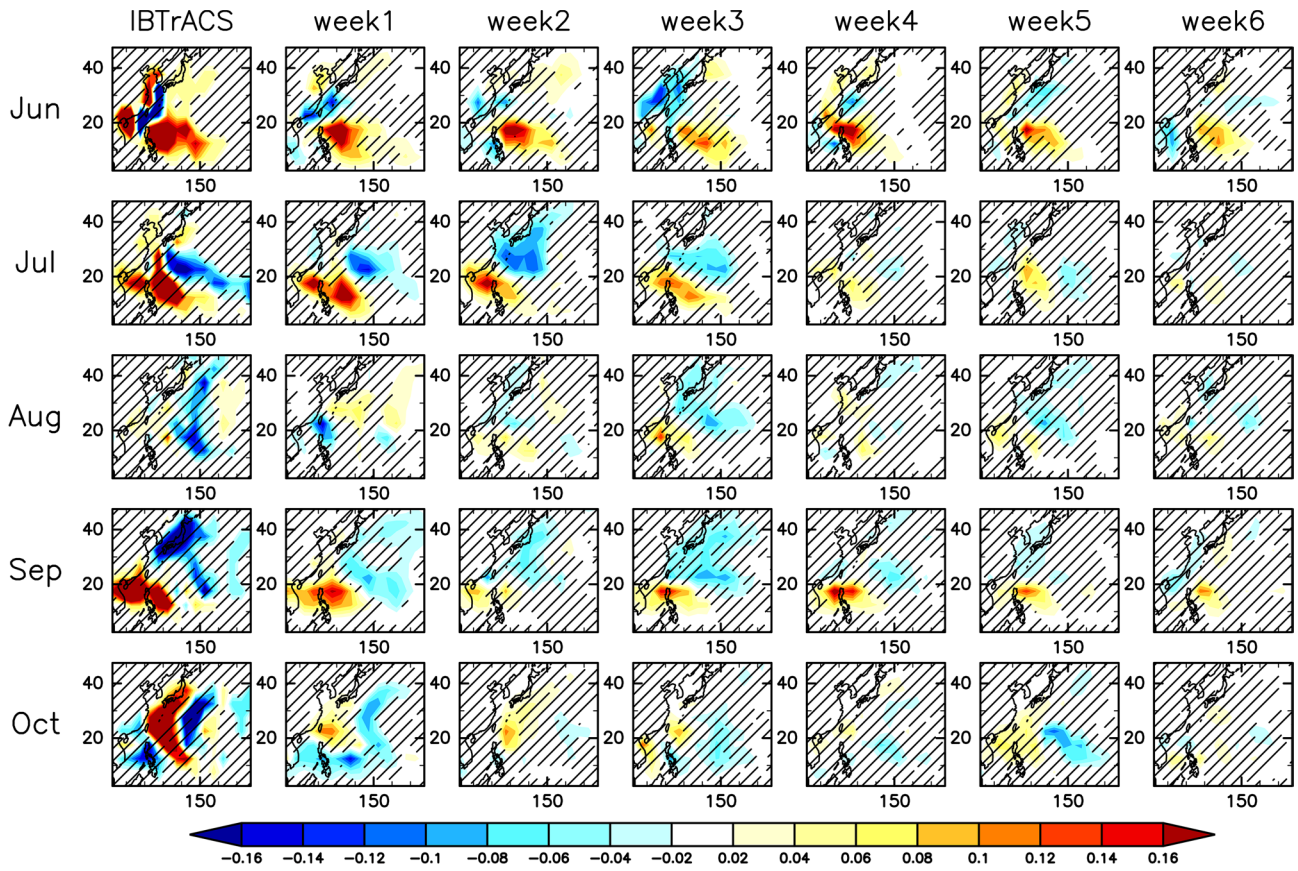

Figure 1. The monthly difference in the normalised TC track density between the enhanced (5–8) and suppressed (1–4) BSISO phases in the WNP (day^{-1}). The uppermost panels are for June and the lowermost panels are for October. The leftmost panels show the best track data, with the ECMWF model with forecast lead times of 1–6 weeks arrayed to the right. The area without hatch indicates where the null hypothesis (that the difference is zero) is rejected at a 90% significance level according to the bootstrap method with sampling repeated 10,000 times. BSISO, boreal summer ISO; ECMWF, European Centre for Medium-Range Weather Forecasts; WNF, western North Pacific.

(northwestward) by the beta effect. We also assume TCs do not die out until they reach the boundary of the analysis area (0–60°N, 100–180°E). ERA-Interim data (Dee et al., 2011) were used to estimate the observed steering flow.

3. Results

3.1. Impact of the BSISO on the TC Tracks

Figure 1 shows the difference in the normalised TC track densities between the enhanced and suppressed BSISO phases in the WNP. In the observations (Figure 1, leftmost panels), the BSISO significantly influences the TC tracks but its effect varies based on the region and month. In June, TCs formed in the enhanced BSISO phases are more likely to hit the Philippines, China and Korea and less likely to hit Taiwan and western Japan than those formed in the suppressed BSISO phases. In July, TCs formed in the enhanced BSISO phases are more likely to hit China and the Philippines and less likely to move south of Japan. In August, the difference is not significant over the analysis area. In September, TCs formed in the enhanced BSISO phases are more likely to hit the Philippines and South China and less likely to hit Japan. In October, interestingly, the tendencies are virtually reversed: TCs formed in the enhanced BSISO phases are more likely to hit Japan and less likely to hit the Philippines and South China.

Despite the number of TCs being much higher in the ECMWF model because of the 11-member ensemble, the model simulates a similar distribution of the differences in the TC track density to the observations at forecast lead times of up to a week, in which the model error is small. This result indicates that the observed

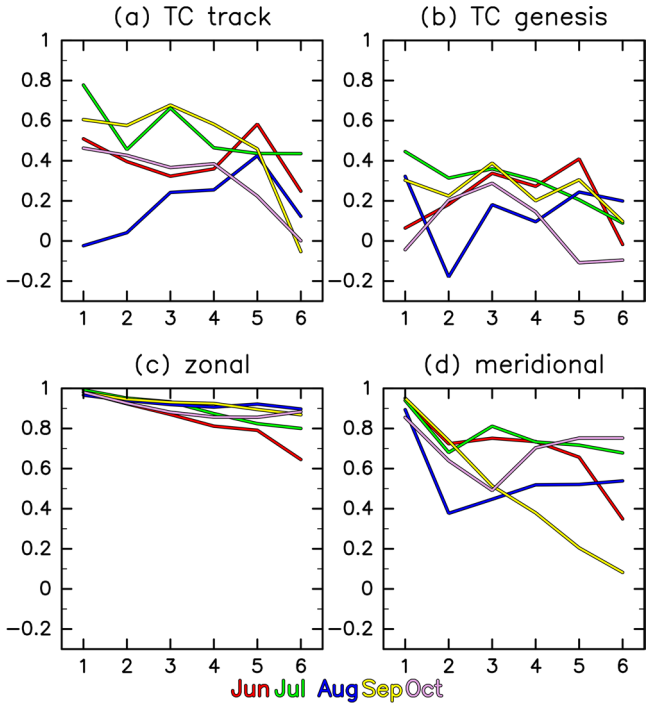

Figure 2. The spatial correlation coefficient (*y*-axis) between the observations and the ECMWF model of the (a) normalised TC genesis frequency, (b) normalised TC genesis density and (c) zonal and (d) meridional components of the steering flow in the analysis area (0–50°N, 100–180°E) for each forecast lead time (*x*-axis in weeks). ECMWF, European Centre for Medium-Range Weather Forecasts.

impact of the BSISO on the normalised TC track density is robust. In addition, the ECMWF model successfully reproduces the impact of the BSISO on the TC track up to a month in advance, especially for July and September. The model performance is, however, low, especially in August (Figures 1 and 2a). In general, the difference becomes less clear and the model performance deteriorates as the forecast lead time increases except for August. In August, the model performance improves along with the forecast lead time, but the correlation is still quite low (~0.4 at week 5). Because almost all regions showed that the observed differences in the TC track density were statistically insignificant (the third raw of Figure 1), this may have been influenced by under-sampling of the observation data.

3.2. Cause of Model Error

The error in the impact of the BSISO on the TC tracks should originate from those of the TC genesis location and/or the steering flow. Figure S1 shows the monthly difference in the normalised TC genesis density between the enhanced and suppressed BSISO phases. The observed difference in the TC genesis frequency is different from the TC track density even at low latitudes (Figure 1). This result suggests that the differences in both the TC genesis density and the steering flow contribute to that in the TC track density. In June, July, and September, more TCs form south of 20°N and less TCs form north of 20°N in the enhanced BSISO phases. The active TC formation region is collocated with the active convection region and the inactive TC formation region is collocated with the inactive convection region in the enhanced BSISO phases (Figure S2). The ECMWF model qualitatively reproduced these different distributions of TC genesis well in July and September but with less accuracy as the forecast lead time increases. The active convection region is slightly tilted to the south with longitude in the observation data and week 1 of the model but this becomes a west-east orientation as the forecast lead time increases. Moreover, the inactive convection region north of the active convection becomes unclear. These model biases for the convective activity may contribute to the biases in the TC genesis distribution in July and September. Conversely, in August and October, the observed differences do not have a well-defined pattern, which is probably hard to reproduce in the model. As for the steering flow, Figure S3 shows the monthly differences in the steering flow between the enhanced and suppressed BSISO phases. In general, the westerly anomaly is large in the southern Philippines and extends east up to 150°E. A large easterly anomaly can be seen near 20°N in June—July and September. This anomaly shifts northward (near 30° N) in August. These anomalies are related to the eastward extension of the monsoon trough in the enhanced phases of the BSISO. The extension enhances the low-level large-scale vorticity. Thus, TCs are more likely to form along the shear line lying between the westerly and easterly anomalies (Figure S1) (Nakano et al., 2015; Yoshida et al., 2014), and those TCs tend to be translated by stronger easterlies at low latitudes as observed in June, July, and September (Figure 1). Features of the steering flow anomaly at low latitudes are relatively well simulated in the ECMWF model. At midlatitudes, the anomalies of both the zonal and meridional components are complex. For example, an anticyclonic anomaly can be found just south of Japan in July and the anomalous flow significantly meanders east of Japan in September. These anomalous flows in the model became weak and zonal with longer forecast lead times.

To summarize, Figures 2b–2d show the spatial correlations between the observations and the model data of the difference in the TC genesis density and the zonal and meridional components of the steering flow between the enhanced and suppressed BSISO phases, respectively, as a function of the forecast lead time in the analysis area, which is the same as shown in Figure 1 (0–50°N, 100–180°E). In general, the correlation of the TC genesis density is the lowest, ranging from 0.4 to −0.2, and that of the zonal component of the steering flow is the highest, ranging from 1 to 0.7. The correlation of the meridional component of the steering flow is between these ranges (ranging from 1 to 0.1). These results suggest that the error in the TC genesis

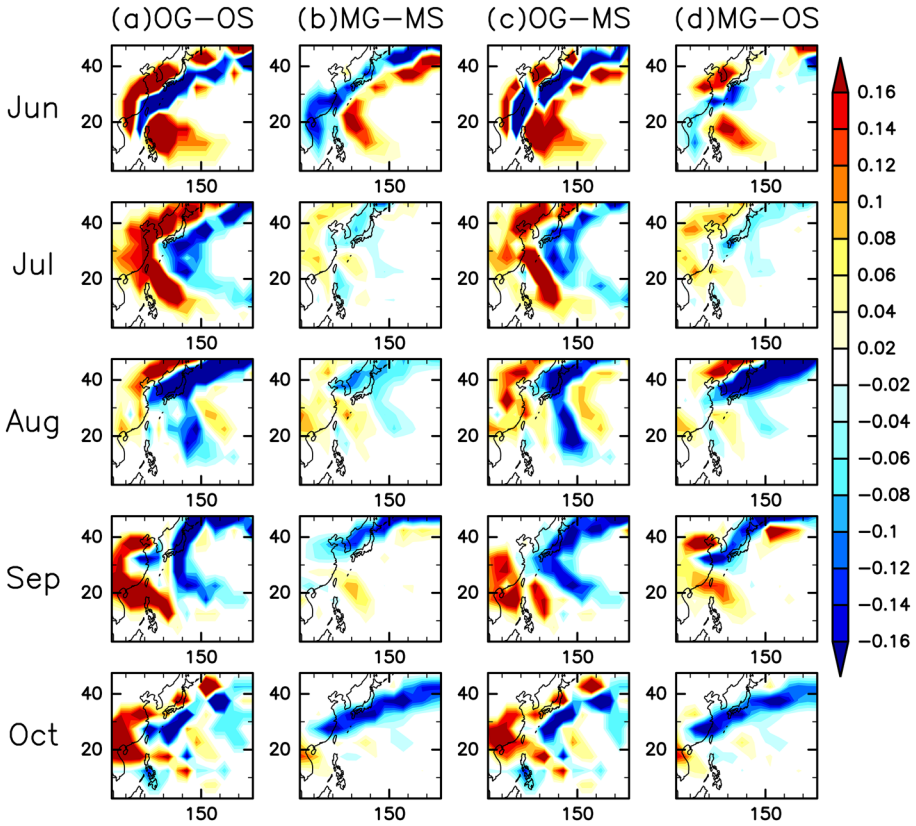

Figure 3. BAM results using observed (O)/modeled (M) TC genesis (G)/Steering flow(S) in the months of June (uppermost)−October (lowermost). BAM, beta and advection model.

density largely contributes to the error in the TC track density. In other words, model performance for TC genesis density for each month would result in the different prediction skill for each month.

To investigate this point further, four sensitivity experiments, OG-OS, MG-MS, MG-OS, and OG-MS, were conducted using BAM. Here "O," "M," "G," and "S" stand for observed, modeled, genesis and steering flow, respectively. For example, in the OG-OS experiments, which imitate the observations, BAM advects TCs from the observed position of TC formation using the observed monthly mean steering flow. In the MG-MS experiments, which imitate the ECMWF model, BAM advects TCs from the modeled position of TC formation in the ECMWF model using the monthly mean steering flow simulated in the ECMWF model. The MG-OS and OG-MS experiments were conducted to examine the impacts of the ECMWF model on TC formation and steering flow, respectively.

Figure 3 shows the results of the experiments for week 6. Note that the results are qualitatively the same for other forecast lead times (not shown). Interestingly, OG-OS (Figure 3a) qualitatively reproduced the observed impact of BSISO on the TC tracks well except for October (see the left panels of Figure 1), despite the TCs being advected by the monthly mean steering flow, ensuring that the BAM is useful for our purpose in general. This also supports the idea that the BSISO affects the likelihood of the TC track pattern. The MG-MS experiments (Figure 3b) show a weak impact of the BSISO on the TC tracks, as analyzed in the ECMWF model data analysis (Figure 1). The OG-MS experiments (Figure 3c) show qualitatively similar results to those of the OG-OS experiments (Figure 3a), especially south of 35°N. The MG-OS experiment (Figure 3d) shows qualitatively similar results to those of the MGMS experiments (Figure 3b). These results suggest that model errors in the differences in the BSISO impact on the TC genesis location cause larger errors in the differences in the TC tracks between the enhanced and suppressed BSISO phases than does the steering flow. In October, a high-speed steering flow (>15 m s^{-1}) region, which is associated with the subtropical jet intrudes south of 30°N (Figure S4). The interaction between TCs and transient eddies at midlatitudes (e.g., baroclinic waves), which are not able to be represented by the monthly mean field used in the BAM, are

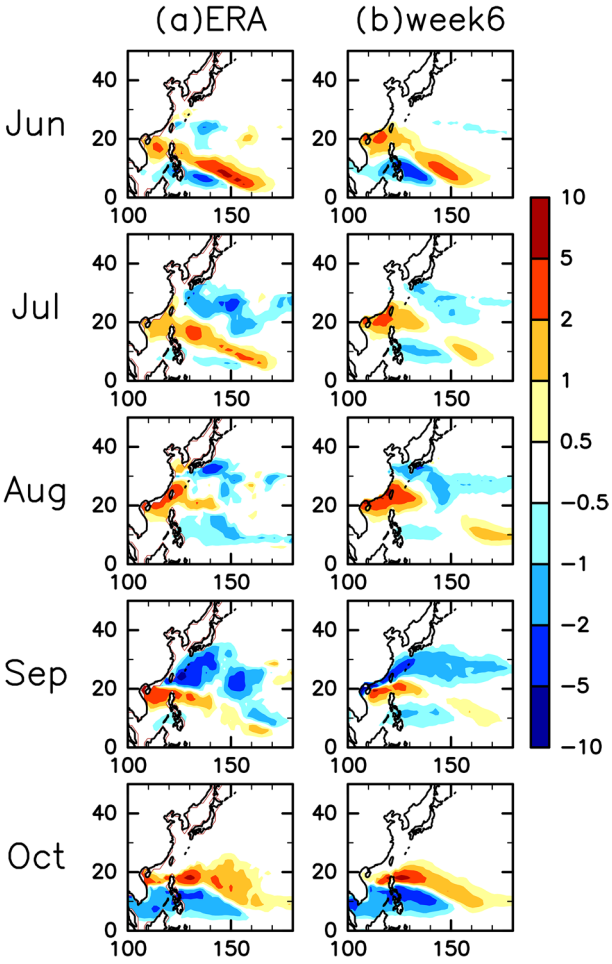

Figure 4. Monthly difference in GPI between the enhanced and suppressed phases of the BSISO analyzed in (a) ERA and (b) the ECMWF model at a forecast lead time of 6 weeks of June (uppermost)–October (lowermost). BSISO, boreal summer ISO; ECMWF, European Centre for Medium-Range Weather Forecasts.

more likely happen. Thus, the BAM probably cannot properly simulate the impact of the BSISO on TC track in that month.

4. Summary and Discussion

In this study, the impact of BSISO on the TC tracks and how the tracks are simulated in the ECMWF model were investigated. The TC tracks were significantly influenced by the BSISO state, and the way that BSISO affects the TC tracks showed regional and seasonal variations (Figure 1). For example, the normalised TC track density (i.e., normalised by the TC number) in the enhanced BSISO phases tends to be significantly higher in the seas adjacent to the northern Philippines throughout the TC season. Conversely, the track density around Japan displays a pronounced seasonal dependence: it is significantly lower in September, while it is higher in October. The ECMWF model successfully reproduced these features with up to a month lead time, especially in July and September (Figure 2). To investigate which model error contributes to that of the TC track, the spatial correlations of the TC genesis density and the steering flow between the observations and the model were examined. The result suggested that the major source of model error for the TC track density results from errors in the TC genesis density. The source of the model error for the TC tracks was further investigated using BAM. The results confirmed that the error in the TC genesis density distribution is the major source of error in the TC track density (Figure 3).

Previous studies showed that differences in the genesis potential index (GPI; Emanuel & Nolan 2004) can represent the differences in the TC genesis density for some long-time scale phenomena, such as the El Nino Southern Oscillation (Camargo, Emanuel, et al. 2007; Camargo, Robertson, et al. 2007) and the intraseasonal oscillation (Camargo et al. 2009). Therefore, the question arises as to whether the model can reproduce differences in GPI between the enhanced and suppressed BSISO phases. Figure 4 shows the monthly difference in GPI between the enhanced and suppressed BSISO phases in the observations and the model at a lead time of 6 weeks. The model reproduced the observed distribution of the difference in GPI even for a forecast lead time of 6 weeks. The difference in GPI reflects the difference in the TC genesis density to some degree in June, July, and September; GPI is higher in the enhanced BSISO phases in June from the South China Sea to east of the Philippines. In addition, in July and September, GPI is lower north of the higher GPI area, as can be seen in the difference in the TC genesis density between the enhanced and suppressed BSISO phases. Even though the difference in GPI has some structure in August and October, the difference in the TC genesis does not display well-defined patterns (Figure S1). More recently, Moon et al. (2018) proposed the intraseasonal GPI and found that the midtropospheric upward motion anomaly associated with the BSISO is correlated well with the boreal summer TC genesis density anomaly. Because large-scale midtropospheric upward motion is usually collocated with active convection region, relationship between the OLR anomaly and normalized TC genesis density anomaly for the enhanced and suppressed phases of BSISO is examined (Figure S2). As seen in the GPI analysis, the OLR anomaly does not represent the TC genesis density anomaly in August and October. These results indicate that the difference in GPI is not always suitable to estimate the modulation of TC genesis by the BSISO, especially in August and October.

The GPI estimates the favourability of TC formation using large-scale environmental parameters (e.g., low-level vorticity, mid-level relative humidity, the deep-layer vertical shear of the horizontal wind and the maximum potential intensity, which reflects the vertical thermodynamic structure of the atmosphere). However, answering the question "why is the GPI unable to represent the TC genesis density anomaly in

some months?" is beyond the scope of the present study but it is noteworthy that TCs form from tropical disturbances (e.g., mixed Rossby-gravity waves or tropical depressions; Takayabu & Nitta, 1993) as well as extratropical systems (e.g., upper tropospheric cold lows; Fudeyasu & Yoshida, 2019). Indeed, Fudeyasu and Yoshida (2019) showed that the number of TC geneses from the upper tropospheric cold lows is the highest in August. Yoshida and Fudeyasu (2020) found that the frequency of the easterly wave flow pattern, which often transforms into tropical depressions, is the highest in October. Considering the small number of tropical disturbances that transform into TCs, we need to understand how the activity of seeds of TC and their survival rate (the fraction of TC formation to tropical disturbances; Lee et al., 2020; Sugi et al., 2020; Yamada et al., 2021) are modulated by the BSISO and improve the model performance of TC genesis predictions based on this understanding.

Data Availability Statement

The S2S ECMWF reforecast data and ERA-interim data can be obtained from the ECMWF's meteorological archive (MARS; https://apps.ecmwf.int/datasets/). NOAA Interpolated OLR data were provided by NOAA/OAR/ESRL PSL, Boulder, Colorado, USA, from their website at https://psl.noaa.gov/data/gridded/data.interp_OLR.html. All figures were drawn using the GFD Dennou Club Library (http://www.gfd-dennou.org/library/dcl/).

Acknowledgments
This study was conducted during MN's visit at ECMWF supported by JAMSTEC. This study was partly supported by JSPS KAKENHI Grant Number JP17K13010 and JAMSTEC-IPRC collaborative Research (JICore). KK acknowledges the support of NOAA CPO Grant NA17OAR4310250. School of Ocean and Earth Science and Technology contribution 11310 and International Pacific Research Centre contribution 1514.

References

Camargo, S. J., Emanuel, K. A., & Sobel, A. H. (2007). Use of a genesis potential index to diagnose ENSO effects on tropical cyclone genesis. *Journal of Climate*, *20*(19), 4819–4834. https://doi.org/10.1175/JCLI4282.1

Camargo, S. J., Robertson, A. W., Gaffney, S. J., Smyth, P., & Ghil, M. (2007). Cluster analysis of typhoon tracks. Part II: Large-scale circulation and ENSO. *Journal of Climate*, *20*(14), 3654–3676. https://doi.org/10.1175/JCLI4203.1

Camargo, S. J., Wheeler, M. C., & Sobel, A. H. (2009). Diagnosis of the MJO modulation of tropical cyclogenesis using an empirical index. *Journal of the Atmospheric Sciences*, *66*(10), 3061–3074. https://doi.org/10.1175/2009JAS3101.1

Colbert, A. J., & Soden, B. J. (2012). Climatological variations in north atlantic tropical cyclone tracks. *Journal of Climate*, *25*(2), 657–673. https://doi.org/10.1175/JCLI-D-11-00034.1

Dee, D. P., Uppala, S. M., Simmons, A. J., Berrisford, P., Poli, P., Kobayashi, S., et al. (2011). The ERA-Interim reanalysis: Configuration and performance of the data assimilation system. *Quarterly Journal of the Royal Meteorological Society*, *137*, 553–597. https://doi.org/10.1002/qj.828

Emanuel, K. A., & Nolan, D. S. (2004). Tropical cyclone activity and global climate. In *Preprints, 26th Conference on Hurricanes and Tropical Meteorology* (pp. 240–241). American Meteorological Society.

Fudeyasu, H., & Yoshida, R. (2019). Statistical analysis of the relationship between upper tropospheric cold lows and tropical cyclone genesis over the western North Pacific. *Journal of the Meteorological Society of Japan*, *97*, 439–451. https://doi.org/10.2151/jmsj.2019-025

Harr, P. A., & Elsberry, R. L. (1991). Tropical cyclone track characteristics as a function of large-scale circulation anomalies. *Monthly Weather Review*, *119*(6), 1448–1468. https://doi.org/10.1175/1520-0493(1991)119<1448:TCTCAA>2.0.CO;2

Harr, P. A., & Elsberry, R. L. (1995). Large-scale circulation variability over the tropical western North Pacific. Part I: Spatial patterns and tropical cyclone characteristics. *Monthly Weather Review*, *123*(5), 1225–1246. https://doi.org/10.1175/1520-0493(1995)123<1225:LSCVOT>2.0.CO;2

Hirata, H., & Kawamura, R. (2014). Scale interaction between typhoons and the North Pacific subtropical high and associated remote effects during the Baiu/Meiyu season. *Journal of Geophysical Research: Atmospheres*, *119*, 5157–5170. https://doi.org/10.1002/2013JD021430

Holland, G. J. (1983). Tropical cyclone motion: Environmental interaction plus a beta effect. *Journal of the Atmospheric Sciences*, *40*(2), 328–342. https://doi.org/10.1175/1520-0469(1983)040<0328:TCMEIP>2.0.CO;2

Jiang, X., Li, T., & Wang, B. (2004). Structures and mechanisms of the northward propagating boreal summer intraseasonal oscillation*. *Journal of Climate*, *17*(5), 1022–1039. https://doi.org/10.1175/1520-0442(2004)017<1022:SAMOTN>2.0.CO;2

Kawatani, Y., Ninomiya, K., & Tokioka, T. (2008). The North Pacic subtropical high characterized separately for June, July, and August: Zonal displacement associated with submonthly variability. *Journal of the Meteorological Society of Japan*, *86*, 505–530. https://doi.org/10.2151/jmsj.86.505

Kikuchi, K. (2021). The boreal summer intraseasonal oscillation (BSISO): A review. *Journal of the Meteorological Society of Japan*, *99*. https://doi.org/10.2151/jmsj.2021-045

Kikuchi, K., & Wang, B. (2010). Formation of tropical cyclones in the Northern Indian Ocean associated with two types of tropical intraseasonal oscillation modes. *Journal of the Meteorological Society of Japan*, *88*(3), 475–496. https://doi.org/10.2151/jmsj.2010-313

Kikuchi, K., Wang, B., & Kajikawa, Y. (2012). Bimodal representation of the tropical intraseasonal oscillation. *Climate Dynamics*, *38*, 1989–2000. https://doi.org/10.1007/s00382-011-1159-1

Klotzbach, P. J. (2014). The Madden-Julian oscillation's impacts on worldwide tropical cyclone activity. *Journal of Climate*, *27*(6), 2317–2330. https://doi.org/10.1175/JCLI-D-13-00483.1

Knapp, K. R., Kruk, M. C., Levinson, D. H., Diamond, H. J., & Neumann, C. J. (2010). The International Best Track Archive for Climate Stewardship (IBTrACS): Unifying tropical cyclone best track data. *Bulletin of the American Meteorological Society*, *91*, 363–376. https://doi.org/10.1175/2009BAMS2755.1

Lee, C.-Y., Camargo, S. J., Sobel, A. H., & Tippett, M. K. (2020). Statistical-dynamical downscaling projections of tropical cyclone activity in a warming climate: Two diverging genesis scenarios. *Journal of Climate*, *33*(11), 4815–4834. https://doi.org/10.1175/JCLI-D-19-0452.1

Li, R. C. Y., & Zhou, W. (2013). Modulation of Western North Pacific Tropical cyclone activity by the ISO. Part II: Tracks and landfalls. *Journal of Climate*, *26*(9), 2919–2930. https://doi.org/10.1175/JCLI-D-12-00211.1

Liebmann, B., Hendon, H. H., & Glick, J. D. (1994). The relationship between tropical cyclones of the Western Pacific and Indian Oceans and the Madden-Julian Oscillation. *Journal of the Meteorological Society of Japan*, *72*(3), 401–412. https://doi.org/10.2151/jmsj1965.72.3_401

Liebmann, B., & Smith, C. (1996). Description of a complete (interpolated) outgoing longwave radiation dataset. *Bulletin of the American Meteorological Society*, *77*(6), 1275–1277.

Marks, D. G. (1992). The beta and advection model for hurricane track forecasting. *NOAA Technical Memorandum NOS-NGS*, *70*, 89.

Moon, J.-Y., Wang, B., Lee, S.-S., & Ha, K.-J. (2018). An intraseasonal genesis potential index for tropical cyclones during Northern Hemisphere summer. *Journal of Climate*, *31*, 9055–9071. https://doi.org/10.1175/JCLI-D-18-0515.1

Nakano, M., Sawada, M., Nasuno, T., & Satoh, M. (2015). Intraseasonal variability and tropical cyclogenesis in the western North Pacific simulated by a global nonhydrostatic atmospheric model. *Geophysical Research Letters*, *42*, 565–571. https://doi.org/10.1002/2014GL062479

Nakazawa, T. (2006). Madden-Julian oscillation activity and typhoon landfall on Japan in 2004. *SOLA*, *2*, 136–139. https://doi.org/10.2151/sola.2006-035

Sugi, M., Yamada, Y., Yoshida, K., Mizuta, R., Nakano, M., Kodama, C., & Satoh, M. (2020). Future changes in the global frequency of tropical cyclone seeds. *SOLA*, *16*, 70–74. https://doi.org/10.2151/sola.2020-012

Takayabu, Y. N., & Nitta, T. (1993). 3-5 Day-Period Disturbances Coupled with Convection over the Tropical Pacific Ocean. *Journal of the Meteorological Society of Japan*, *71*(2), 221–246. https://doi.org/10.2151/jmsj1965.71.2_221

Vitart, F. (2009). Impact of the Madden Julian oscillation on tropical storms and risk of landfall in the ECMWF forecast system. *Geophysical Research Letters*, *36*, L15802. https://doi.org/10.1029/2009GL039089

Vitart, F., Anderson, J. L., & Stern, W. F. (1997). Simulation of interannual variability of tropical storm frequency in an ensemble of GCM integrations. *Journal of Climate*, *10*(4), 745–760. https://doi.org/10.1175/1520-0442(1997)010<0745:SOIVOT>2.0.CO;2

Vitart, F., Ardilouze, C., Bonet, A., Brookshaw, A., Chen, M., Codorean, C., et al. (2017). The subseasonal to seasonal (S2S) prediction project database. *Bulletin of the American Meteorological Society*, *98*(1), 163–173. https://doi.org/10.1175/BAMS-D-16-0017.1

Wang, B., & Rui, H. (1990). Synoptic climatology of transient tropical intraseasonal convection anomalies: 1975–1985. *Meteorology and Atmospheric Physic*, *44*, 43–61. https://doi.org/10.1007/BF01026810

Wang, B., & Xie, X. (1997). A model for the boreal summer intraseasonal oscillation. *Journal of the Atmospheric Sciences*, *54*(1), 72–86. https://doi.org/10.1175/1520-0469(1997)054<0072:AMFTBS>2.0.CO;2

Weare, B. C., & Nasstrom, J. S. (1982). Examples of extended empirical orthogonal function analyses. *Monthly Weather Review*, *110*(6), 481–485. https://doi.org/10.1175/1520-0493(1982)110<0481:EOEEOF>2.0.CO;2

Yamada, Y., Satoh, C. M., Sugi, M., Roberts, M. J., Mizuta, R., Noda, A. T., et al. (2021). Evaluation of the contribution of tropical cyclone seeds to changes in tropical cyclone frequency due to global warming in high-resolution multi-model ensemble simulations. *Progress in Earth and Planetary Science*, *8*, 11. https://doi.org/10.1186/s40645-020-00397-1

Yoshida, R., & Fudeyasu, H. (2020). How Significant are low-level flow patterns in tropical cyclone genesis over the Western North Pacific? *Monthly Weather Review*, *148*, 559–576. https://doi.org/10.1175/MWR-D-19-0023.1

Yoshida, R., Kajikawa, Y., & Ishikawa, H. (2014), Impact of Boreal summer intraseasonal oscillation on environment of tropical cyclone genesis over the Western North Pacific. *SOLA*, *10*, 15–18. https://doi.org/10.2151/sola.2014-004